Structural characterization and energy performance of novel hybrid PVT solar-panels through 3-D FEM and CFD simulations

María Herrando[a], Alba Ramos[b], Ignacio Zabalza[c] and Christos N. Markides[d]

[a] Clean Energy Processes (CEP) Laboratory, Department of Chemical Engineering, Imperial College London, London, United Kingdom, maria.herrando11@imperial.ac.uk
[b] Clean Energy Processes (CEP) Laboratory, Department of Chemical Engineering, Imperial College London, London, United Kingdom, a.ramos-cabal@imperial.ac.uk
[c] University of Zaragoza-CIRCE Institute, Zaragoza, Spain, izabal@unizar.es
[d] Clean Energy Processes (CEP) Laboratory, Department of Chemical Engineering, Imperial College London, London, United Kingdom, c.markides@imperial.ac.uk (CA)

Abstract:

Hybrid Photovoltaic-Thermal (PVT) panels generate both power and heat from the same area with overall efficiencies up to 70%. This work assesses the performance of novel hybrid PVT solar panels considering alternative geometries and materials that maximize heat transfer while allowing weight and cost reductions. A three-dimensional (3-D) model previously developed and validated using 3-D Finite-Element and Computational Fluid-Dynamics (FEM and CFD) software is used for this purpose. The most promising configurations and materials for the absorber-exchanger unit of the proposed PVT panel are studied to analyse their energy performance and behaviour in terms of a thermal-stress assessment. Apart from an assessment of the steady-state performance, for the type of solar PVT panels considered, especially those made of polymeric materials, it is important to evaluate the thermal expansion that the collector suffers, so as to verify whether the associated thermal stresses and strains are within the limits that guarantee a proper performance during its lifetime. The most promising PVT panel is then integrated within a Solar Combined Heat and Power (S-CHP) system for power and heating provision to a single-family house located in Zaragoza (Spain), in order to assess its daily energy performance through transient simulations on half-hourly basis. The results show that these novel polymeric PVT panel configurations are a promising alternative to commercial PVT panel designs, achieving an improved thermal performance compared to a reference case (4% higher optical efficiency and 15% lower heat loss coefficient), while suffering lower strains in most of the PVT layers. Furthermore, the novel polycarbonate 3×2 mm flat-box configuration has the potential to cover, on average, around 50% of the total space heating and Domestic Hot Water (DHW) demand and around 87% of the total electricity demand (including lighting, cooling and home appliances).

Keywords:

Absorber-exchanger unit; Computational Fluid-Dynamics; Energy demand; Finite-Element Method; Hybrid PVT; Solar Combined Heat and Power; Thermal expansion.

1. Introduction

Solar energy is an abundant, inexhaustible and clean energy resource. Currently, the most widespread and mature solar-energy technologies are solar Photovoltaic (PV) systems and solar-thermal systems. PV systems convert ~15-20% of the incident solar radiation, while rejecting the remaining 80-85% in the form of wasted heat and which, if recovered, could be used to heat a circulating fluid such as air or water [1]. This has been the main motivation behind the development of hybrid PVT systems, which generate both power and heat from the same area with overall efficiencies up to 70% [2]. In particular, PVT-water (PVT-w) systems are considered an interesting option for the combined provision of space heating and Domestic Hot Water (DHW) in the residential sector, which accounts for 25% of the total electricity and 30% of the final energy consumption in the EU [3]. Furthermore, the cooling of the PV panel allows these PVT-w systems to maintain PV efficiencies of around 15% [1]. An added advantage of these systems is the more efficient use of roof space compared to stand-alone PV and solar-collector systems [4].

Previous research undertaken by the authors [1,5] concluded that commercially available PVT-w systems can cover up to 50% of the total electricity demand and between 35-50% of the DHW demand of a typical household located in London (UK), while completely covering the electricity demand and around 70% of the DHW demand if located in a household in Larnaca (Cyprus) [6]. However, despite its potential, there are still very few companies worldwide commercializing this type of panel [7], with most of the products available on the market not having optimized designs for PVT applications. For this reason, the International Energy Agency (IEA), in its Task 35 for the development of PVT systems, insists on the need to optimize these systems from both manufacturing and technical performance points of view, by developing projects that accelerate their economic viability to compete with current renewable energy technologies. Specifically, as other authors concluded [2,8], further research in the thermal absorber of the PVT collector is required, particularly on the design and materials of new thermal absorber collectors, with the aim of optimizing the structural and geometrical parameters that enhance the performance of current PVT units [9].

With this in mind, the main aim of the present research is to characterize promising hybrid PVT configurations, as identified in previous research [10], by focusing on the thermal expansion that the collector suffers and the associated thermal strains, and by verifying that the stresses are below materials' limits. A second aim is to assess the energy performance of the most promising PVT configuration, as well as a reference case (commercial PVT panel), when it is integrated in a Solar Combined Heat and Power (S-CHP) system (including thermal storage) that provides heat and power to a single-family house. To this end, the electrical (including lighting, cooling and home appliances) and thermal (including space heating and DHW) demands of a single-family house located in Zaragoza (Spain) are estimated with the software *EnergyPlus* [11], and then fed to a 1-D model of the S-CHP system. Based on the specifications of the S-CHP system configuration (number of PVT units, collector flow-rate, storage tank dimensions, etc.), the model outputs, among others, the electricity and hot water generated throughout a day on a half-hourly basis, which is then used to calculate the percentage of the household's energy demand covered by the S-CHP system.

2. Hybrid PVT panel selection

The two main components of the PVT panel are the PV module and thermal collector, which can be further divided into the glazing, the thermal absorber and the riser water tubes (referred to, in the present work, as the absorber-exchanger unit) and the insulation layer (see Fig. 1).

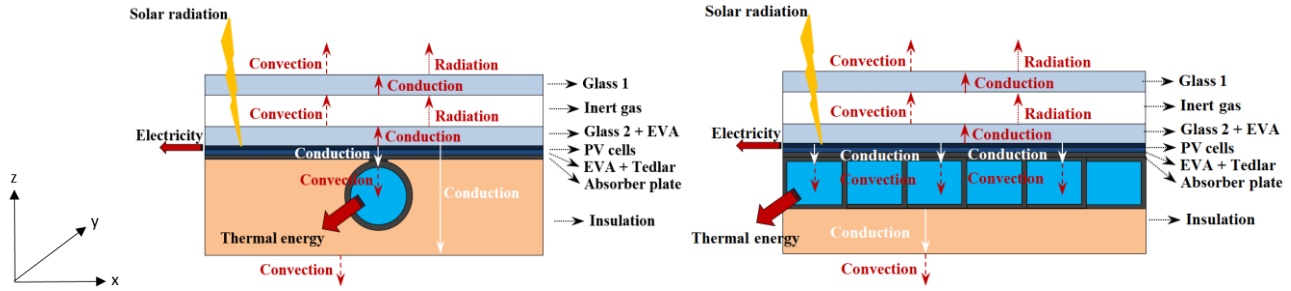

Fig. 1. PVT collector cross-section for the (left) parallel tubes (sheet-and-tube) and (right) flat-box structure configuration, showing the various collector layers (not to scale).

The most widespread absorber-exchanger configuration for PVT water units studied so far is copper parallel tubes (sheet-and-tube) [1,12-16], which is also used in various commercially available PVT panels. However, in this configuration, the collector fin efficiency and the tube bonding quality are crucial design factors that limit the heat than can be extracted, which restraints the overall efficiency that can be achieved [17]. Consequently, several authors [14,15] made significant efforts to optimize the design of sheet-and-tube collectors. In an attempt to overcome this problem, other authors [12,17-22] proposed a flat-box structure (square or rectangular channels) to improve the fin efficiency and bonding quality, increasing significantly the heat transfer area between the absorber plate and the cooling fluid (see Fig. 1 right). Some studies [12,17,20] have considered this absorber-exchanger

configuration made of extruded aluminium alloy, while other authors [18,21,22] proposed the use of Polycarbonate (PC) to lower the price and cost of the PVT unit.

The present work is focused on the flat-box structure, since previous research undertaken by the authors [10] indicated that improved heat transfer and higher efficiencies can be achieved with this absorber-exchanger configuration. The preliminary results obtained showed that rectangular channels improve the thermal performance of the PVT unit compared to the a reference case (commercial copper parallel tubes PVT collector), achieving up to around 5% higher optical efficiency and up to about 16% lower heat loss coefficient, while also lowering the weight (up to 12%) and investment costs (up to 22%) of the PVT panel. From the different materials and channel dimensions modelled in the aforementioned study, Table 1 shows the most promising configurations which are selected in this research to assess their mechanical and energy performance through 3-D FEM and CFD simulations.

Table 1. Summary of the materials and dimensions studied for the absorber-exchanger unit.

Copper	Aluminium	Polycarbonate (PC)	Polyamide PA30-33[†]
S&T_D8-n9*	S&T_D8-n9	3×2 mm	3×2 mm
3×2 mm[+]	3×2 mm	6×4 mm	
		10×10 mm	

**Sheet-and-Tube (S&T) collector with external diameter (D =) 8 mm and (n =) 9 riser tubes*

[+]Rectangular channels of cross-sectional dimensions: Width × Height (W×H)

[†]PA30-33 stands for Polyamide Zytel® RS LC3030 NC010 with a load of hexagonal Boron Nitride of 33.33% vol.

A parallel copper-tube PVT collector design (S&T_D8-n9 in Table 1) is used as reference case, representing the commercially available ECOMESH panel [23]. A previous study conducted by the authors showed that the same configuration constructed from aluminium alloy is an interesting alternative since, even though the thermal performance is slightly worse due to the lower conductivity of aluminium, the lower cost of the material leads to lower investment costs and lower payback. A parallel study [10] concluded that among the different flat-box configurations modelled, the range of materials and channel dimensions did not significantly affect the thermal performance of the PVT collector. A maximum variation of 5% in the thermal efficiency curves was observed between the best material (copper) and worst material (polyamide, PA), while a 2.5% variation was observed between the smallest (3×2 mm) and largest (40×10 mm) channel dimensions. The study concluded that the most promising material seems to be polycarbonate (PC), due to its lower price compared to polymers with loading of additives (such as polyamide loaded with hexagonal Boron Nitride (hBN) particles, like the one considered in this work, PA30-33 [24]).

Therefore, from the 18 different flat-box configurations modelled in the previous study [10], three different channel dimensions (3×2 mm, 6×4 mm and 10×10 mm) (made from the same material, PC) are selected to study their influence on the thermal expansion of the PVT panel, and four different materials (copper, aluminium, PC and PA30-33) are considered with the same channel dimensions (3×2 mm (W×H), as the most promising one), to assess the influence of the material.

3. Methodology

In this work, a 3-D FEM and CFD model of a PVT unit previously developed in COMSOL, and validated in previous work [10], is further developed to include thermal expansion and associated strains due to temperature gradients. The most promising PVT configurations are integrated in an also validated 1-D model with the experimental results of a commercial PVT panel provided by the panel manufacturer, EndeF Engineering [23]. This 1-D model has been developed in the EES software environment, and consists of a S-CHP system that contains a water pump, bypass, thermal storage and auxiliary heater required to satisfy the energy (both heating and electricity) demands of a single-family house (see Fig. 3). The daily energy performance of this system is then analysed, so as to estimate the percentage of the energy demand than can be covered in the case scenario proposed (single-family semi-detached house, with 2 floors with an area of ~55 m^2 each, U-value of the façade 0.35 W/(m^2 K), double-glazed windows, located in Zaragoza, Spain).

3.1. Simulation models

For the purpose of this study, two different models are considered: i) a detailed 3-D model of the PVT unit, and ii) a simplified 1-D model of a S-CHP system. For the PVT unit, all the layers above the absorber plate are the same, varying only the absorber-exchanger unit with the configurations detailed in Table 1, which are defined by geometrical parameters and material properties. The energy balance of the whole PVT panel is then resolved in both models considering radiation, convection and conduction heat exchanges among the layers.

Both the 1-D and 3-D models are developed under the following assumptions: i) the solar radiation is absorbed only by the collector [25] and the absorption in the cover glass and in the frame is neglected, ii) the ambient temperature is considered uniform around the module [26,27] and heat losses from the sides of the collector are negligible [27], iii) the solar irradiance and wind speed are uniform over the panel surface, iv) the temperature dependence of the material properties of the solid components is neglected, v) the water mass flow-rate is distributed uniformly among all riser tubes [26,28], vi) free convection in the tubes is neglected, and vi) lateral radiative thermal exchanges between the solar collector fluid channels are neglected [15,26,29,30].

3.1.1. 3-D PVT panel modelling

As mentioned above, the different absorber-exchanger configurations were modelled in a previous study [10] using the same models applied to each specific geometry as that used as a basis for a 3-D thermodynamic PVT model (sheet-and-tube) validated against commercial data. In this work, the 3-D FEM and CFD modelling goes one step further and the solid mechanics physic is added to undertake a structural analysis. Due to the significant amount of both time and computational resources required for detailed 3-D FEM-CFD simulations, especially in problems involving multi-physics processes such as in hybrid PVT panels, some simplifications are applied to simplify the problem (even though this slightly reduces the accuracy of the 3-D model as discussed below). As stated previously, it is assumed that the water mass flow-rate is divided equally among all tubes of the collector [26,28], such that symmetry can be used to simplify this problem. Thus, only two channels are modelled, reducing significantly the computational time and resources. To verify that the number of modelled channels do not influence the results, simulations were run with 2, 5, 10 and 15 channels, obtaining the same results (within numerical error), when the same boundary conditions were applied.

The structural analysis is simplified into a 2-D problem in the *yz* plane as the most important thermal expansion and associated stresses are expected on the flow direction, *y* axis, due to the temperature gradient and on the *z* axis due to gravity. In Fig. 2 (left) it can be observed that the *y* axis corresponds to the flow direction and *z* axis to the vertical plane. In Fig. 2 (right) a 3-D view of the 2-channel PVT collector modelled in COMSOL is shown; note that the collector is tilted 35°.

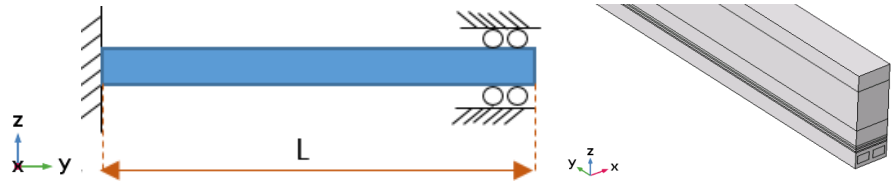

Fig. 2. (left) Illustration of the PVT collector (of length L) supports at the inlet (fixed) and outlet (prescribed displacement), and (right) 3-D model of two 3×2 mm channel PVT collector.

With regards to the slightly reduced accuracy due to the model simplification mentioned above, the authors have verified that this is a conservative analysis through a simplified 3-D model which showed that in reality, when considering the full 3-D problem, the maximum stresses suffered by the PVT unit are lower than those obtained here. Regarding the boundary conditions, it is assumed that the PVT collector is completely fixed with the frame at the collector water inlet, while at the collector water outlet the frame has some tolerance, allowing expansion in the flow direction (*y* axis) but not allowing displacement on the *z* axis (see Fig. 2 left). The authors are aware of the limitations of this model, so it is expected that a full 3-D model of the whole collector with the most promising configuration will be undertaken in a wider structural analysis in future work.

In the 3-D model, all the PVT configurations detailed in Table 1 are studied at steady-state with the same initial conditions, detailed in Table 2. It should be noted that two collector flow-rates are considered: i) the nominal flow-rate according to the PVT manufacturer [23] of the reference case for the sheet-and-tube configurations, 30 L/h (8.3×10^{-3} kg/s), and ii) the optimum flow-rate for the flat-box structure according to Cristofari et al. [26,21] for all flat-box configurations, 19.2 L/h (5.3×10^{-3} kg/s).

Table 2. Initial conditions and other important constant system parameters.

G_i	Incident solar irradiance	1000	W/m^2
T_a	Ambient temperature	25	°C
T_{in}	Inlet water temperature	20.2	°C
$\dot{m}_c$	Collector flow-rate – sheet-and-tube configuration	8.3×10^{-3}*	kg/s
$\dot{m}_c$	Collector flow-rate – flat-box configuration	5.3×10^{-3}†	kg/s
β	Collector tilt angle	35	°

**Normal operation water flow-rate provided by the PVT manufacturer* [23]
†Optimum flow-rate for the 10×10mm flat-box configuration according to Cristofari et al. [26,21]

Finally, a dynamic diurnal simulation was undertaken in COMSOL for the most promising absorber-exchanger configuration and for the reference case (S&T_D8-n9). The objective was to verify that the dynamics of the PVT panel are faster than the time steps selected for the overall S-CHP system analysis in the 1-D model (see Section 3.1.2). To this end, the same 3-D model was run as time dependent with the solar irradiance varying with time ($G_i = f(t)$), and at steady-state with the solar irradiance corresponding to each half-hour time step. The same results were obtained in both cases (within numerical error), as expected, so it can be concluded that dynamic fluctuations for a sunny day (as the ones considered in the present study) do not affect steady-state calculations with the time step selected for the 1-D analysis (30 min).

3.1.2. 1-D S-CHP system

A 1-D quasi steady-state model of a complete S-CHP system has been developed in the software EES to assess the energy performance of the novel absorber-exchanger configurations of the PVT panels proposed in this research. The model integrates the governing equations of the PVT unit following the ASHRAE method [31] which includes the PVT geometry (such as fin efficiency (F), heat removal factor (F_R), the overall heat loss coefficient (U_L), etc.), adapted also for the flat-box structure. As shown in Fig. 3, the S-CHP system comprises an active closed-loop system in which, in normal operation, the collector outlet flow enters the heat exchanger located inside the storage tank, heats the water in the tank, exits the tank and returns to the inlet of the solar collector to be heated again. A bypass valve is required to control the temperature of the water leaving the collector and entering the tank to ensure that this stream only heats (and does not cool) the water in the storage tank. This bypass is controlled by a differential on/off solenoid valve that sends the collector fluid flow to the tank only when the outlet flow temperature from the collector is greater than the temperature of the water in the storage tank. If this is not the case, the fluid is returned to the collector via the bypass connection for further heating.

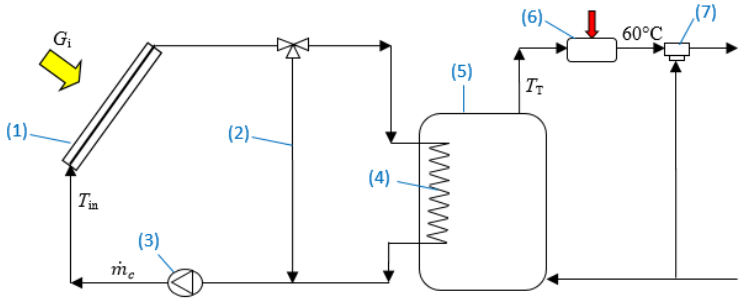

Fig. 3. Schematic diagram of the S-CHP system: (1) PVT unit, (2) by-pass, (3) water pump, (4) tank heat exchanger, (5) water storage tank, (6) auxiliary heater, (7) mixing device for final temperature delivery regulation (not considered in this work).

A reference house has also been modelled in *EnergyPlus* [11] to estimate the energy demand throughout a day (including electricity for lighting, cooling and household appliances, and natural gas for space

heating and DHW). The half-hourly results are then fed to the 1-D model, which provides as outputs (at each time step), among others, the temperatures of the different layers of the PVT collector, the collector water outlet temperature, the water storage tank temperature, the energy (electricity and hot water) generated by the S-CHP system and the percentage of energy demand covered.

3.2. PVT unit parameters

The PVT unit taken as the reference case and modelled is the commercially available ECOMESH panel [23] which consists of (from top to bottom): a Transparent Insulating Cover (TIC) comprising a transparent cover (glass) and an insulating gas [32], a poly-crystalline (pc-Si) PV module, an EVA encapsulating film, an absorber-exchanger unit (which transforms the solar radiation to heat and transfers it to the collector fluid), and a layer of insulation material at the bottom (see Fig. 1 left). The absorber-exchanger unit consists of a sheet-and-tube heat exchanger in which water flows in (nine) copper parallel pipes [3], and an equivalent unit but made of aluminium alloy is also studied (see Table 1). The rest of alternatives studied consist of a flat-box absorber-exchanger unit with rectangular channels of cross-sectional dimensions and materials as detailed in Table 1 above. Table 3 summarizes the physical and mechanical properties of different PVT layers and thermal absorber materials considered in this research.

Table 3. Physical and mechanical properties of the different materials considered.

Properties	Density (ρ) (kg/m^3)	Thermal Conductivity (k) (W/(m·K))	Heat capacity (c_p) (J/(kg·K))	Young's modulus (GPa)	Poisson's ratio (-)	Thermal Expansion Coefficient ×10^{-6} (1/K)	Yield Stress (MPa)	Ultimate Tensile Stress (MPa)
Tempered Glass[1]	2,210	1.4	730	70	0.22	9	750-2,130	180
EVA[2]	960	0.35	2,090	0.018	0.32	350	-	26
Tedlar[3]	1,250	0.36	1,200	2.34	0.4	75	38	55-110
PV module (Silicon)[4]	2,329	130	700	170	0.28	2.6	3,200-3,460	160-180
Copper[5]	8,700	400	385	110	0.35	17	230	287
Aluminium alloy[4]	2,702	237	903	75	0.33	22.2	265	300
PC[6]	1,180	0.775	1,200	2.35	0.38	68	59-70	55-75
PA30-33[7]	1,390	3.6	1,700	2.9	0.36	50.9	50-95	90-165

[1][33]; [2][34]; [3][35]; [4][36];[5][37];[6][38];[7][24]

The aim of the structural analysis is to evaluate whether the different PVT layers will yield when subjected to the strains associated with thermal expansion due to temperature changes in normal operating conditions. To this end, the von Mises stress criterion is used (also called the equivalent or effective stress) [39-41]. The von Mises stress criterion can be formulated as indicated in (1), and it can be defined as the driving force for damage in many ductile engineering materials:

$$\sigma_M = \sqrt{\frac{1}{2}\cdot\left[\left(\sigma_x-\sigma_y\right)^2+\left(\sigma_x-\sigma_z\right)^2+\left(\sigma_y-\sigma_z\right)^2+6\cdot\left(\tau_{xy}+\tau_{yz}+\tau_{xz}\right)\right]}. \quad (1)$$

The von Mises stress is routinely computed by COMSOL, and it is compared to the material's yield stress (or to the Ultimate Tensile Stress (UTS) when it is lower than the former, see Table 3), to determine whether each layer would yield or fracture. The maximum displacement due to deformation that the PVT unit suffers is also analysed; in this case this is defined as the percentage of the maximum displacement suffered by the PVT collector over the total collector length.

4. Results and discussion

4.1. PVT panel structural analysis

As mentioned previously, each of the absorber-exchanger configurations defined in Table 1 were implemented in COMSOL with the different physics involved (heat transfer, laminar flow and solid mechanics). The 3-D models were then run at steady-state with the initial conditions detailed in Table

2. Detailed results of the performance curve for each of the PVT configurations studied are not presented here due to space limitations, however further details can be found in the previous study [10]. The present work focusses on the structural analysis of the most promising configurations, as detailed below.

Table 4 summarizes the maximum values of von Mises stress for the different layers of the PVT configurations, providing an overview of which layers are suffering more strains. In addition, the stress distribution throughout the layer surface, which allows the identification of the critical points, is also obtained, as shown in the following figures.

Table 4. Maximum values of von Mises stress (MPa) for the different layers of the PVT configurations.

Layers	Glass 1	Glass 2	PV top	PV back	Tedlar-EVA	Absorber surface	Absorber cross-sectional end
Cu-S&T_D8-n9	10.19	31.14	23.20	24.05	9.53	57.09	102.25
Al-S&T_D8-n9	10.61	33.43	26.71	27.97	9.63	49.92	89.58
PC-Box_3×2	8.50	29.26	31.87	33.57	5.19	8.27	8.33
PC-Box_6×4	8.84	28.91	34.27	36.00	5.03	7.91	8.03
PC-Box_10×10	8.55	28.05	36.68	38.42	4.92	7.76	8.24
Cu-Box_3x2	8.46	29.05	30.10	31.46	6.83	55.67	85.20
Al-Box_3x2	8.47	29.09	35.97	38.05	6.69	50.66	77.07
PA30-33-Box_3×2	8.48	28.82	29.38	30.82	5.37	9.76	10.09

By comparing the von Mises stress in the different PVT layers with their corresponding yield or UTS, based on the most restrictive value for each particular case, it is possible to conclude that no yield or fracture is expected in any of the layers. For the cover and inner glasses, the maximum von Mises stress is lower than 6% and 19% of the UTS, respectively. In terms of stress distribution throughout the layers' surfaces, the results obtained show that in all PVT configurations, the maximum von Mises stress for the cover glass (Glass 1) occurs at the collector water inlet, which is attributed to its weight effect at the tilted angle. Meanwhile, the maximum value for the inner glass (Glass 2) occurs at the end of the collector, where the maximum thermal expansion occurs.

For the PV layer, the maximum von Mises stresses are between 14% to 23% of its UTS, being the worst case the PC 10×10 mm flat-box configuration, which can be attributed to the higher thermal expansion suffered on the *z* axis compared to the rest of alternatives. It is observed that for the polymeric (PC and PA30-33) flat-box configurations, the layer that suffers the highest strains is the PV panel, with higher von Mises stress values than for the sheet-and-tube collector. This is attributed to the larger buckling of the former configurations, especially in the *z* axis, as shown in Fig. 4. Specifically, the critical point occurs in a section towards the collector fluid outlet as indicated in Fig. 4 (see vertical arrow). This figure shows the PV layer buckling throughout its length; which is the same as for the whole PVT collector since all layers are assumed to be maintained in contact (except for the cover glass). Regarding the variation of the strains for the PC flat-box configurations with different channel dimensions, Table 4 shows that the von Mises stress increases with the channel dimensions, together with the thermal expansion that the PVT collector suffers (from 0.6% to 0.8% displacement in the *z* axis respect to the total length, and from 0.04% to 0.07% in the *y* axis).

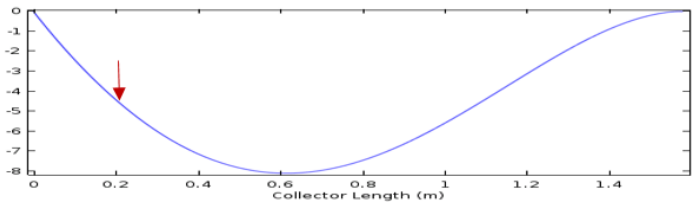

Fig. 4. Thermal expansion of the PV layer in the z axis (mm) throughout its length for the PC 3×2 mm PVT collector. The vertical arrow indicates the location of the maximum von Mises stress.

Finally, concerning the absorber-exchanger unit, the most critical configuration in terms of strains suffered is the sheet-and-tube collector, in which the maximum von Mises stress is around 64% and 56% of the yield stress for the copper and aluminium configurations respectively. As shown in Fig. 5, the maximum stress occurs in the bonding between the absorber layer and the riser pipe at the

collector water outlet. This result is expected since: i) this is the area where the highest temperatures are reached, and ii) stress is concentrated in a very small surface area compared with the rest of the PVT layers. As consequence, the sheet-and-tube configuration is the one with the highest strains.

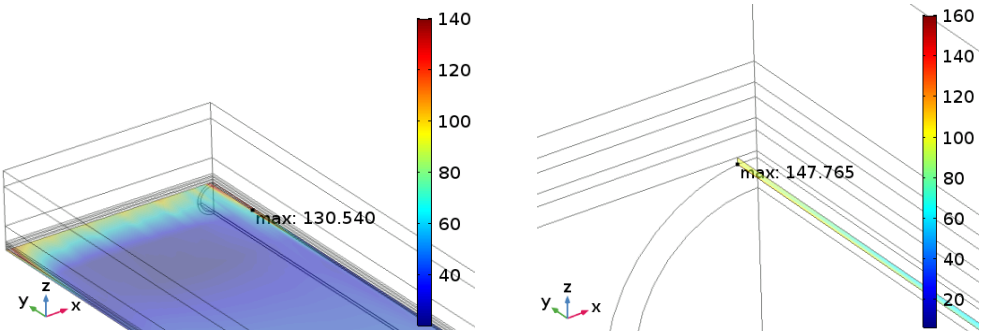

Fig. 5. Von Mises Stress (MPa) in the absorber layer in the (left) lower part at the end of the collector, and (right) lateral surface of the bond between absorber and pipe, for the sheet-and-tube copper PVT collector.

It should be noted that the values of the mechanical properties can vary within a wide range depending on the specific copper and aluminium alloys used for the bonding in each case, so more accurate values (provided by the sheet-and-tube collector manufacturer) are necessary for a more detailed structural analysis. In all of the absorber-exchanger flat-box configurations, the maximum von Mises stress within the absorber-exchanger unit is located in the cross-sectional area at the collector outlet (see Fig. 6), and amounts to < 37% of the yield stress of the metal (copper, aluminium) collectors and < 13% of the yield stress of the polymeric collectors. Additionally, as shown in Table 4 and Fig. 6, the maximum overall collector strains in the copper and aluminium flat-box configurations occur in the aforementioned absorber-exchanger cross-sectional area at the collector water outlet, together with the maximum thermal expansion on the *y* axis.

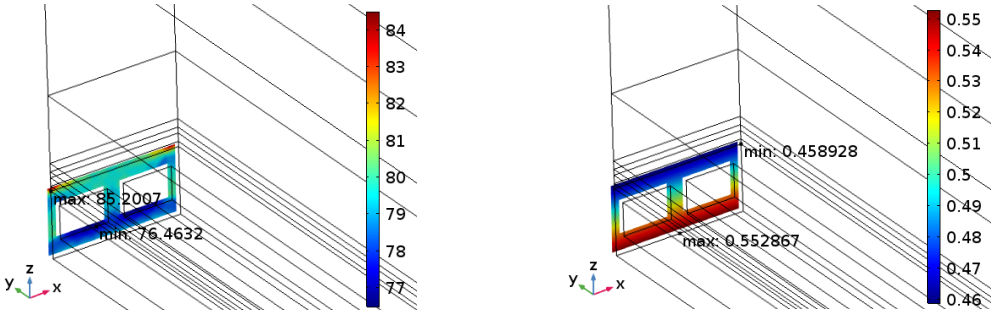

Fig. 6 (left) Von Mises stress (MPa) and (right) thermal expansion in the y axis (mm) over the cross-sectional area of the absorber-exchanger unit for the copper flat-box 3×2 mm configuration.

4.2. S-CHP system energy performance analysis

Bearing in mind the above structural analysis and the results obtained in previous research [10], the most promising flat-box configuration, with PC 3×2 mm channels, was integrated with a complete S-CHP system in order to analyse its daily energy performance and to compare this with the benchmark reference case (commercial sheet-and-tube PVT collector). To this end, the same system specifications were set in both configurations, 10 PVT collectors connected in parallel (15 m^2 total aperture area) integrated with a 1000-L water storage tank. To estimate the energy demand, a single-family semi-detached house was modelled in *EnergyPlus* software, implementing the occupancy profiles and schedules to calculate the electricity consumption for lighting, cooling and household appliances, and natural gas consumption for space heating and DHW. The weather conditions of Zaragoza (Spain) were selected for the calculations and the solar irradiance and ambient temperature provided by the software were input in the 1-D S-CHP system. The household energy demands (electricity and natural gas) were estimated on a half-hourly basis and used as inputs to the 1-D model.

The daily results over two different days (one in winter and in summer) are presented in Figs 7 and 8. Two different flow-rates per collector were selected to adjust the PVT system performance

according to the household energy needs: i) 30 L/h in winter, and ii) 75 L/h in summer, as recommended by the PVT manufacturer of the benchmark reference case [42].

It should be noted that in order to calculate the net electricity (E_{net}) at each time step, the energy required to run the water pump of the S-CHP system is considered. Negative values of E_{net} means that there is a deficit of electricity (that should be bought from the grid), while positive values means that there is a surplus of electricity that could be either stored or sold to the grid (see Figs 7 and 8). Similar results are obtained for both the reference (S&T) case and the PC 3×2 mm flat-box collector, with slightly better results for the latter, as expected, since the improvement in the performance curve of the flat-box absorber-exchanger configuration compared to the reference case is moderate (4% higher optical efficiency and 15% lower heat loss coefficient).

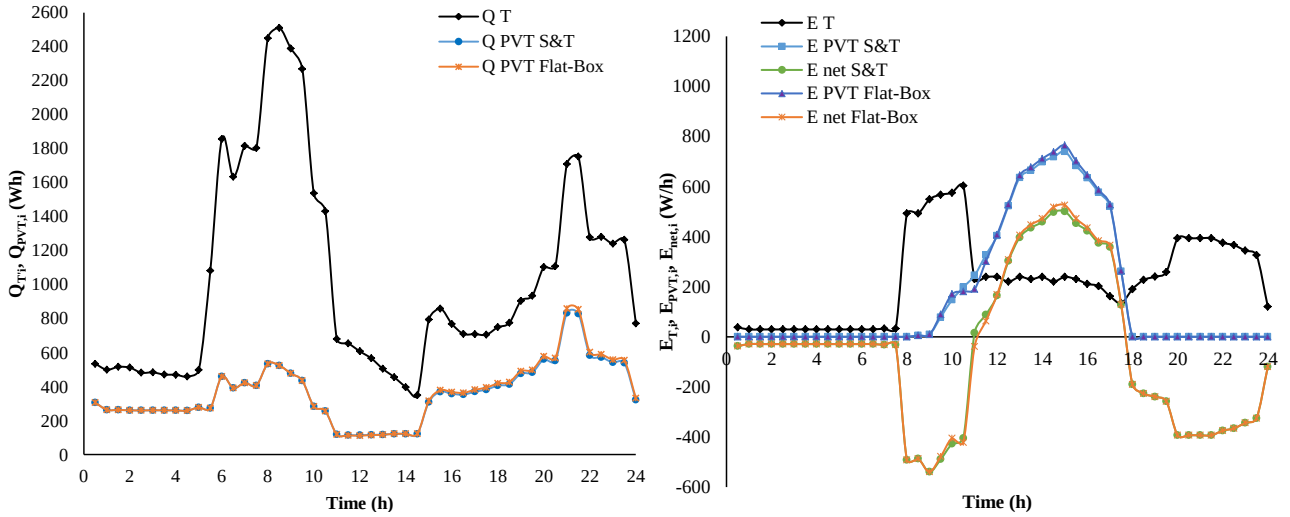

Fig. 7. (left) Total household space heating and DHW demand (Q_T) and space heating and DHW demand covered (Q_{PVT}); and (right) total household electricity demand (E_T), electricity generated (E_{PVT}) and net electricity (E_{net}) by the reference (S&T) and PC 3×2 mm flat-box PVT systems in a winter day in Zaragoza (Spain).

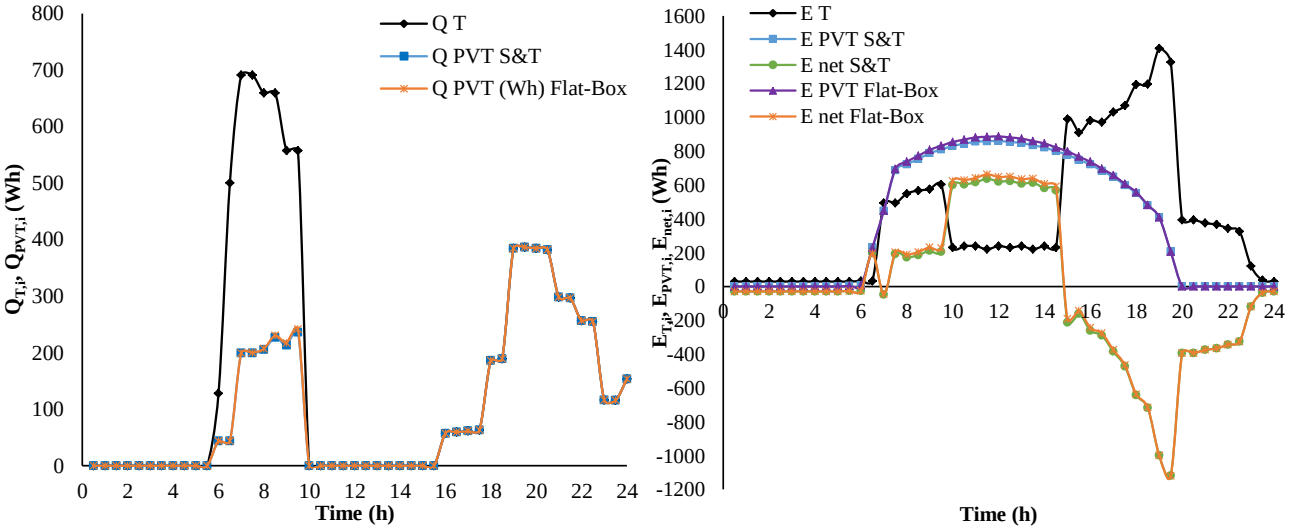

Fig. 8. (left) Total household DHW demand (Q_T) and DHW demand covered (Q_{PVT}); and (right) total household electricity demand (E_T), electricity generated (E_{PVT}) and net electricity (E_{net}) by the reference (S&T) and PC 3×2 mm flat-box PVT systems in a summer day in Zaragoza (Spain).

The results show that on a sunny day in winter it is possible to cover 35% and 36% of the thermal (including space heating and DHW), while also covering 75% and 76% of the electricity demand with the S&T and flat-box PVT collectors respectively (see Fig. 7). On the other hand, on a summer day it is possible to cover 62% of the DHW demand (since there is no space heating) for both collectors, and 96% and 98% of the electricity demand with the S&T and flat-box PVT collectors respectively (see Fig. 8). The peak of electricity demand in summer occurs between 15-20h (Fig. 8-

right), due to the cooling demand. It should be noted that in summer the percentage of DHW demand that can be covered is limited by the fact that the maximum DHW consumption occurs early in the morning when the PVT system is not operating (see Fig. 8-left), so the amount of DHW that can be supplied by the PVT system depends on the temperature of the tank at the beginning of the day. However, as the model was run in a daily basis, the water tank temperature at the beginning of the day does not consider the temperature reached in the tank at the end of the previous day, so it is expected that a higher percentage of the demand can be covered by these S-CHP systems.

5. Conclusions

Based on a number different PVT configurations for the absorber-exchanger unit previously studied [10], this work proceeds to consider the most promising ones (plus a benchmark reference case), which are selected for structural and daily performance characterization. The study is focused on the flat-box structure since preliminary results have shown that this novel configuration improves the thermal performance of the PVT unit compared to a benchmark reference case (sheet-and-tube collector) by up to about 5% in terms of improved optical efficiency and about 16% in terms of reduced heat losses, while lowering the weight (up to 12%) and investment costs (up to 22%) of the panel [10]. Specifically, three different channel dimensions ($W \times H$ = 3×2, 6×4 and 10×10 mm) made from the same material (PC), and four different materials (copper, aluminium, PC and PA30-33) with the same channel dimensions (3×2 mm, as the most promising one) are studied.

A structural analysis is performed in COMSOL, on a previously developed and validated 3-D FEM and CFD thermal-fluid model of PVT collectors. The results show that the novel PVT configurations proposed in this research seem a very promising alternative to the reference sheet-and-tube collector, since apart from the aforementioned advantages: i) in general, the maximum von Mises stresses suffered by the different PVT layers in the flat-box configurations are lower than for the sheet-and-tube collector; furthermore, ii) even though the buckling suffered by the flat-box configurations is higher (up to around 90% higher in the worst case, PC 10×10 mm configuration), the displacement in the *z* axis (vertical axis) is only 0.8% respect to the total length in that case. Therefore, these novel flat-box configurations are not expected to suffer higher strains than the commercially available PVT units, but they are expected to achieve higher thermal efficiencies at lower investment costs.

To complement the previous study [10], the most promising flat-box configuration, namely with PC 3×2 mm channels, and the benchmark reference case (commercial sheet-and-tube PVT collector) are integrated within a whole S-CHP system (bypass, thermal storage, household energy demand, etc.) in a 1-D model developed in the EES, in order to assess the energy performance of these PVT units when installed in a single-family semi-detached house located in Zaragoza (Spain). The household energy demand (including electricity consumption for lighting, cooling and household appliances, and natural gas consumption for space heating and DHW) is modelled in *EnergyPlus* and fed to the 1-D S-CHP model so as to estimate the daily fraction of energy demand that can be covered on a half-hourly basis. The results show that with the novel PVT configuration it is possible to cover 36% of the space heating and DHW demands, while covering 76% of the electricity demand on a sunny day in winter, and 62% of the DHW demand (as there is no space heating) and 98% of the electricity demand on a sunny day in summer. Therefore, it can be concluded that the polymeric flat-box configuration is a promising alternative to commercial PVT panels.

Nevertheless, further work is required to: i) analyse in detail the structural and energy performance of the whole PVT unit in the 3-D FEM and CFD model to consider also the effect of the PVT collector sides (both in terms of energy losses and structural analysis), ii) assess the energy performance of the overall S-CHP system throughout the whole year, and iii) optimize the S-CHP system parameters (such as PVT collector flow-rate, number of PVT units, water tank size, etc.) to maximize the percentage of household's energy demand covered throughout a year.

Acknowledgments

This work was undertaken as part of the PhD Program 'Renewable Energies and Energy Efficiency' of the University of Zaragoza – CIRCE Research Institute, during the international placement of MH at Imperial College London. This work was supported by the UK Engineering and Physical Sciences Research Council (EPSRC) [grant number EP/M025012/1]. Data supporting this publication can be obtained on request from cep-lab@imperial.ac.uk.

References

[1] Herrando M, Markides CN, Hellgardt K. A UK-based assessment of hybrid PV and solar-thermal systems for domestic heating and power: System performance. Appl Energy 2014;122:288–309.

[2] Michael JJ, Iniyan S, Goic R. Flat plate solar photovoltaic-thermal (PV/T) systems: A reference guide. Renew Sustain Energy Rev 2015;51:62–88.

[3] Antonanzas J, del Amo A, Martinez-Gracia A, Bayod-Rujula AA, Antonanzas-Torres F. Towards the optimization of convective losses in photovoltaic–thermal panels. Sol Energy 2015;116:323–36.

[4] Allan J, Dehouche Z, Stankovic S, Mauricette L. Performance testing of thermal and photovoltaic thermal solar collectors. Energy Sci Eng 2015;3:310–26.

[5] Guarracino I, Mellor A, Ekins-daukes NJ, Markides CN. Dynamic coupled thermal-and-electrical modelling of sheet-and-tube hybrid photovoltaic/thermal (PVT) collectors. Appl Therm Eng 2016;101:778–95.

[6] Guarracino I, Freeman J, Ekins-daukes N, Markides CN. Performance assessment and comparison of solar ORC and hybrid PVT systems for the combined distributed generation of domestic heat and power. Int. Conf. Heat Transf. Fluid Mech. Thermodyn., 2016.

[7] Herrando M, Markides CN. Hybrid PV and solar-thermal systems for domestic heat and power provision in the UK: Techno-economic considerations. Appl Energy 2016;161:512–32.

[8] Fudholi A, Sopian K, Yazdi MH, Ruslan MH, Ibrahim A, Kazem HA. Performance analysis of photovoltaic thermal (PVT) water collectors. Energy Convers Manag 2014;78:641–51.

[9] Zhang X, Zhao X, Smith S, Xu J, Yu X. Review of R&D progress and practical application of the solar photovoltaic/thermal (PV/T) technologies. Renew Sustain Energy Rev 2012;16:599–617.

[10] Herrando M, Guarracino I, del Amo A, Zabalza I, Markides CN. Energy Characterization and Optimization of New Heat Recovery Configurations in Hybrid PVT Systems. ISES Conf. Proc., Palma de Mallorca (Spain): 2016.

[11] EnergyPlus software. https://energyplus.net/ (accessed February 9, 2017).

[12] Chow TT, Ji J, He W. Photovoltaic-Thermal Collector System for Domestic Application. J Sol Energy Eng 2007;129:205.

[13] Tripanagnostopoulos Y, Souliotis M, Battisti R, Corrado A. Energy, cost and LCA results of PV and hybrid PV/T solar systems. Prog Photovoltaics Res Appl 2005;13:235–50.

[14] Zondag HA, de Vries DW, van Helden WGJ, van Zolingen RJC, van Steenhoven AA. The yield of different combined PV-thermal collector designs. Sol Energy 2003;74:253–69.

[15] Chow TT. Performance analysis of photovoltaic-thermal collector by explicit dynamic model. Sol Energy 2003;75:143–52.

[16] Kalogirou SA. Use of TRNSYS for modelling and simulation of a hybrid pv–thermal solar system for Cyprus. Renew Energy 2001;23:247–60.

[17] He W, Chow T, Ji J, Lu J, Pei G. Hybrid photovoltaic and thermal solar-collector designed for natural circulation of water. Appl Energy 2006;83:199–210.

[18] Huang BJ, Lin TH, Hung WC, Sun FS. Performance evaluation of solar photovoltaic / thermal

systems. Sol Energy 2001;70:443–8.

[19] Shan F, Cao L, Fang G. Dynamic performances modeling of a photovoltaic-thermal collector with water heating in buildings. Energy Build 2013;66:485–94.

[20] Chow TT, He W, Ji J. Hybrid photovoltaic-thermosyphon water heating system for residential application. Sol Energy 2006;80:298–306.

[21] Cristofari C, Notton G, Poggi P, Louche A. Modelling and performance of a copolymer solar water heating collector. Sol Energy 2002;72:99–112.

[22] Cristofari C, Canaletti J, Notton G, Darras C. Innovative patented PV/TH Solar Collector: optimization and performance evaluation. Energy Procedia 2012;14:235–40.

[23] EndeF Engineering. Technical Datasheet ECOMESH panel.

[24] Ghaffari Mosanenzadeh S, Liu MW, Osia A, Naguib HE. Thermal Composites of Biobased Polyamide with Boron Nitride Micro Networks. J Polym Environ 2015;23:566–79.

[25] Agarwal RK, Garg HP. Study of a Photovoltaic-Thermal system - Thermosyphonic solar water heater combined with solar cells. Energy Convers Manag 1994;35:605–20.

[26] Cristofari C, Notton G, Canaletti JL. Thermal behavior of a copolymer PV/Th solar system in low flow rate conditions. Sol Energy 2009;83:1123–38.

[27] Notton G, Cristofari C, Mattei M, Poggi P. Modelling of a double-glass photovoltaic module using finite differences. Appl Therm Eng 2005;25:2854–77.

[28] Bhattarai S, Oh J, Euh S, Krishna G, Hyun D. Simulation and model validation of sheet and tube type photovoltaic thermal solar system and conventional solar collecting system in transient states. Sol Energy Mater Sol Cells 2012;103:184–93.

[29] Sandnes B, Rekstad J. A photovoltaic/thermal (PV/T) collector with a polymer absorber plate. Experimental study and analytical model. Sol Energy 2002;72:63–73.

[30] Zondag HA, De Vries DW, Van Helden WGJ, Van Zolingen RJC, van Steenhoven AA. The thermal and electrical yield of a PV-thermal collector. Sol Energy 2002;72:113–28.

[31] ASHRAE Standard. Standard 93-2003: Methods of testing to determine the performance of solar collectors, 2013.

[32] del Amo A, Martínez-Gracia A, Bayod-Rújula AA, Antoñanzas J. An innovative urban energy system constituted by a photovoltaic/thermal hybrid solar installation: Design, simulation and monitoring. Appl Energy 2016.

[33] MakeItFrom.com. Toughened (Tempered) Soda-Lime Glass, http://www.makeitfrom.com/material-properties/Toughened-Tempered-Soda-Lime-Glass (accessed February 7, 2017).

[34] EndeF Engineering. EVASAFE DataSheet, 2017.

[35] GoodFellow. Tedlar - Polyvinylfluoride (PVF), http://www.findtheneedle.co.uk/companies/goodfellow-cambridge-ltd/products/tedlar-polyvinylfluoride-pvf (accessed December 6, 2016).

[36] Cambridge University Engineering Department. Materials data book. Mater Courses, 2003.

[37] Alanod Solar. Copper absorber plate, 2017.

[38] GoodFellow. Polycarbonate - online catalogue source - Goodfellow, http://www.goodfellow.com/E/Polycarbonate.html (accessed December 6, 2016).

[39] Roylance D. Mechanical Properties of Materials. Springer 2008;190:645.

[40] Von Mises R. Mechanik der Festen Korper im Plastisch Deformablen Zustand. Math Phys 1913;1:582–92.

[41] Hjelmstad KD. Fundamentals of Structural Mechanics. Second Edi. Urbana-Champaign, Illinois: Springer US; 2005.

[42] Endef - Energy, Development and Future. http://endef.com/ (accessed February 10, 2017).